

β -Turn and β -Hairpin Mimicry with Tetrasubstituted Alkenes

Robb R. Gardner, Gui-Bai Liang, and Samuel H. Gellman*

Contribution from the Department of Chemistry, University of Wisconsin, Madison, Wisconsin 53706

Received July 13, 1998. Revised Manuscript Received December 30, 1998

Abstract: Synthesis and conformational analysis are reported for molecules containing the *trans*-5-amino-3,4-dimethylpent-3-enoic acid residue (ADPA, **1**). This amino acid is a glycyglycine mimic, in which the central amide group is replaced with an *E*-tetrasubstituted alkene. It was anticipated that this isosteric replacement would promote specific local (β -turn) and nonlocal (β -hairpin) conformational preferences. Previous work has shown that the most common β -turn conformations (type I and type II) are not strong inducers of β -hairpin formation, while the rare “mirror image” β -turns (type I' and type II') promote β -hairpin formation. We therefore sought an achiral unit with a strong turn-forming propensity, since the lack of stereogenic centers within such a unit would eliminate the energetic distinction between common and “mirror image” turn conformations. In the ADPA unit, avoidance of allylic strain was expected to preorganize the backbone for adoption of folded conformations. A combination of NMR and IR data for di-, tri-, and tetrapeptide analogues containing the ADPA residue reveal that β -turn- and β -hairpin-like folding is promoted in methylene chloride solution.

Introduction

There is great interest in peptide analogues that have some or all of the backbone replaced by non- α -amino acid segments.¹ Molecular chimeras of this type may display improved pharmacological properties relative to peptides, e.g., resistance to peptidase degradation, and passive diffusion across biological membranes. A second source of interest is the prospect of diminishing the conformational flexibility that characterizes short α -amino acid oligomers. Backbone rigidification can enhance pharmacological behavior because biological activity usually requires that a peptide or peptide mimic adopt a specific conformation. Peptide mimetic units that provide conformational control can also serve as tools in basic biostructural research, e.g., for construction of model systems that probe the origins of protein folding preferences.²

Here we describe the development of a dipeptide mimic that promotes β -hairpin-like folding when coupled to α -amino acid residues.³ The dipeptide mimic is centered on a tetrasubstituted alkene; this design builds upon the widespread use of alkene units as peptidase-resistant isosteric replacements for backbone amide groups.⁴ We extend beyond these precedents by taking advantage of allylic strain (actually, the avoidance of allylic strain) to induce U-shaped conformations,⁵ which in turn promote β -hairpin-like folding. Wipf et al. have recently reported related studies.^{4e}

A β -hairpin (two strands connected by a short loop) can be viewed as the smallest increment of antiparallel β -sheet secondary structure.⁶ The most common loop contains only two residues, and in this case, the two loop residues are also the two central residues of a β -turn (β -turns are usually defined in terms of four residues⁷). Surveys of β -hairpins in crystalline proteins led Thornton and co-workers to recognize that two rare classes of β -turn, type I' and type II', often form two-residue hairpin loops.^{7a} In contrast, type I and type II β -turns, by far the most common among β -turns in crystalline proteins, are seldom involved in two-residue β -hairpin loops. (β -Turn “types” are defined by the ϕ and ψ torsion angles of the central two residues; the prime (') indicates that all four torsion angles are mirror images of the torsion angles in the unprimed version.⁸) This discovery has prompted several groups to try to stabilize β -hairpin conformations in short peptides by employing loop sequences that are predisposed toward type I' or type II' β -turn conformations.⁹ Our approach has involved use of D-residues to induce loop formation.^{9a–h} We have shown that D-proline at the first of the two loop positions strongly stabilizes β -hairpin conformations of tetrapeptides in organic solvents.^{9a,b} We have subsequently demonstrated that D-proline exerts a similar effect in 12–16 residue peptides in aqueous solution.^{9c–e}

(1) For leading references, see: (a) Ball, J. B.; Alewood, P. F. *J. Mol. Recog.* **1990**, *3*, 55. (b) Giannis, A.; Kolter, T. *Angew. Chem., Int. Ed. Engl.* **1993**, *32*, 1244. (c) Gillespie, P.; Cicariello, J.; Olsen, G. L. *Biopolymers* **1997**, *43*, 191. (d) Hanessian, S.; McNaughton-Smith, G.; Lombart, H.-G.; Lubell, W. D. *Tetrahedron* **1997**, *53*, 12789.

(2) For leading references, see: (a) Kemp, D. S.; Osllick, S. L.; Allen, T. J. *J. Am. Chem. Soc.* **1996**, *118*, 4249. (b) Kemp, D. S.; Bowen, B. R.; Muendel, C. C. *J. Org. Chem.* **1990**, *55*, 4650. (c) Brandmeier, V.; Sauer, W. H. B.; Feigel, M. *Helv. Chim. Acta* **1994**, *77*, 70. (d) Nesloney, C. L.; Kelly, J. W. *J. Am. Chem. Soc.* **1996**, *118*, 5836. (e) Nowick, J. S.; Insaf, S. J. *Am. Chem. Soc.* **1997**, *119*, 10903. (f) Schopfer, U.; Stahl, M.; Brandl, T.; Hoffmann, R. W. *Angew. Chem., Int. Ed. Engl.* **1997**, *36*, 1745. (g) Schneider, J. P.; Kelly, J. W. *Chem. Rev.* **1995**, *95*, 2169. (h) Nowick, J. S.; Smith, E. M.; Pairish, M. *Chem. Soc. Rev.* **1996**, 401.

(3) Preliminary report: Gardner, R. R.; Liang, G.-B.; Gellman, S. H. *J. Am. Chem. Soc.* **1995**, *117*, 3280.

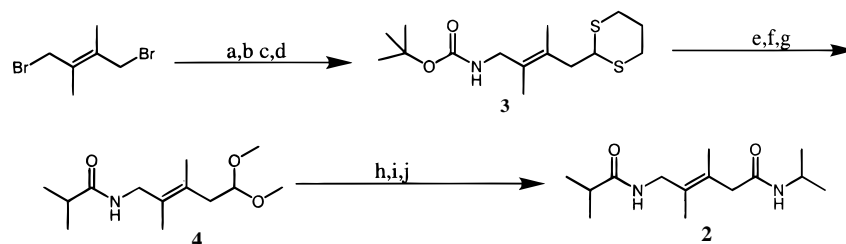
(4) (a) Hann, M. M.; Sammes, P. G.; Kennewell, P. D.; Taylor, J. B. *J. Chem. Soc., Chem. Commun.* **1980**, 234. (b) Cox, M. T.; Heaton, D. W.; Horbury, J. J. *J. Chem. Soc., Chem. Commun.* **1980**, 799. (c) Cox, M. T.; Gormley, J. J.; Hayward, C. F.; Petter, N. N. *J. Chem. Soc., Chem. Commun.* **1980**, 800. (d) Wipf, P.; Fritch, P. C. *J. Org. Chem.* **1994**, *59*, 4875. (e) Wipf, P.; Henninger, T. C.; Geib, S. J. *J. Org. Chem.* **1998**, *63*, 6088.

(5) General discussions of allylic strain: Johnson, F. *Chem. Rev.* **1968**, *68*, 375. Berg, U.; Sandström, J. *Adv. Phys. Org. Chem.* **1989**, *25*, 1. Hoffmann, R. W. *Angew. Chem., Int. Ed. Engl.* **1992**, *31*, 1124. For the use of acyclic stereochemical control to preorganize the backbone of a saturated alkane hairpin mimic, see: Schopfer, U.; Stahl, M.; Brandl, T.; Hoffmann, R. W. *Angew. Chem., Int. Ed. Engl.* **1997**, *36*, 1745.

(6) Gellman, S. H. *Curr. Opin. Chem. Biol.* **1998**, *2*, 717.

(7) (a) Sibanda, B. L.; Thornton, J. M. *Nature* **1985**, *316*, 170. (b) Wilmot, C. M.; Thornton, J. M. *J. Mol. Biol.* **1988**, *203*, 221. (c) Sibanda, B. L.; Thornton, J. M. *J. Mol. Biol.* **1993**, *229*, 428. (d) Mattos, C.; Petsko, G. A.; Karplus, M. *J. Mol. Biol.* **1994**, *238*, 733. (e) Gunasekaran, K.; Ramakrishnan, C.; Balaran, P. *Protein Eng.* **1997**, *10*, 1131.

(8) Rose, G. D.; Gierasch, L. M.; Smith, J. A. *Adv. Protein Chem.* **1985**, *37*, 1 and references therein.

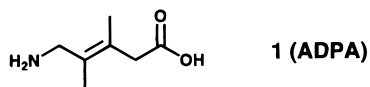
Scheme 1^a

^a Key: (a) 2-Lithio-1,3-dithiane (1 equiv). (b) NaN_3 , Bu_4NBr . (c) Ph_3P , THF (wet). (d) Di-*tert*-butyl dicarbonate. (e) MeSO_3H , MeOH. (f) Isobutyryl chloride, Et_3N . (g) Bis(trifluoromethyl)acetoxyiodobenzene, MeOH. (h) 0.5 M HCl, THF/ H_2O . (i) NaClO_2 , 2-methyl-2-butene. (j) DCC, *N*-hydroxysuccinimide, isopropylamine.

Nonhydrolyzable β -hairpin-promoting dipeptide mimics may be useful to medicinal chemists because compact β -hairpins, with two-residue loops, have been shown to play key roles in protein–protein¹⁰ and protein–RNA¹¹ recognition. Dipeptide mimics of this type may allow construction of metabolically stable antagonists for natural complexation processes. β -Hairpin inducers can also be used to elucidate the sources of β -sheet folding preferences in proteins, if these inducers allow one to stabilize small increments of β -sheet secondary structure in solution.²

Results and Discussion

Design and Synthesis of the Dipeptide Mimic. Trans-disubstituted alkene units have been widely employed as isosteric replacements for the backbone amide groups of peptides because alkenes are inert to peptidases and the trans configuration mimics the conformational preference of a secondary amide.⁴ This substitution does not, however, diminish the conformational flexibility that is characteristic of peptides.¹² We chose to deviate from the typical alkene isostere approach by employing a tetrasubstituted alkene unit because we anticipated that avoidance of allylic strain would limit conformational freedom in a way that favors β -hairpin folding.^{13,14} We selected *trans*-5-amino-3,4-dimethylpent-3-enoic acid (ADPA, **1**), which



mimics glycylglycine, as our initial target. This target has the

(9) Use of D-Pro-Xxx segments to promote β -hairpin formation: (a) Haque, T. S.; Little, J. C.; Gellman, S. H. *J. Am. Chem. Soc.* **1994**, *116*, 4105. (b) Haque, T. S.; Little, J. C.; Gellman, S. H. *J. Am. Chem. Soc.* **1996**, *118*, 6975. (c) Haque, T. S.; Gellman, S. H. *J. Am. Chem. Soc.* **1997**, *119*, 2303. (d) Stanger, H. E.; Gellman, S. H. *J. Am. Chem. Soc.* **1998**, *120*, 4236. (e) Schenck, H. L.; Gellman, S. H. *J. Am. Chem. Soc.* **1997**, *120*, 44869. (f) Awasthi, S. K.; Ragothama, S.; Balaran, P. *Biochem. Biophys. Res. Commun.* **1995**, *216*, 375. (g) Karle, I. L.; Awasthi, S. K.; Balaran, P. *Proc. Natl. Acad. Sci. U.S.A.* **1996**, *93*, 8189. (h) Ragothama, S. R.; Awasthi, S. K.; Balaran, P. *J. Chem. Soc., Perkin Trans. 2* **1998**, 137. Use of the L-Asn-Gly segment to promote β -hairpin formation: (i) Ramirez-Alvarado, M.; Blanco, F. J.; Serrano, L. *Nature Struct. Biol.* **1996**, *3*, 604. (j) de Alba, E.; Jimenez, M. A.; Rico, M. *J. Am. Chem. Soc.* **1997**, *119*, 175. (k) Maynard, A. J.; Searle, M. S. *J. Chem. Soc., Chem. Commun.* **1997**, 1297. (l) Sharman, G. J.; Searle, M. S. *J. Chem. Soc., Chem. Commun.* **1997**, 1955. (m) Griffiths-Jones, S. R.; Maynard, A. J.; Sharman, G. J.; Searle, M. S. *J. Chem. Soc., Chem. Commun.* **1998**, 789. (n) Maynard, A. J.; Sharman, G. J.; Searle, M. S. *J. Am. Chem. Soc.* **1998**, *120*, 1996. (o) Sharman, G. J.; Searle, M. S. *J. Am. Chem. Soc.* **1998**, *120*, 5291. (p) We have recently shown that D-Pro-Gly is a stronger hairpin promoter than L-Asn-Gly (ref 9d).

(10) Strynadka, N. C. J.; Jensen, S. E.; Alzari, P. M.; James, M. N. G. *Nat. Struct. Biol.* **1996**, *3*, 290.

(11) (a) Puglisi, J. D.; Chen, L.; Blanchard, S.; Frankel, A. D. *Science* **1995**, *270*, 1200. (b) Ye, X.; Kumar, R. A.; Patel, D. J. *Chem. Biol.* **1995**, *2*, 827. (c) Varani, G. *Acc. Chem. Res.* **1997**, *30*, 189 and references therein.

virtue that substantial conformational preorganization is anticipated in the absence of asymmetric centers, which simplifies the synthetic challenge. In addition, the distinction between “mirror image” turn conformations (e.g., type I vs type I’ β -turns) becomes irrelevant in an achiral dipeptide mimic like ADPA.

The synthesis of diamide **2**, an end-capped derivative of glycylglycine mimic **1**, began with (*E*)-1,4-dibromo-2,3-dimethyl-2-butene^{15a} (Scheme 1). Treatment of this dibromide with 1 equiv of 2-lithio-1,3-dithiane followed by NaN_3 gave a mixture of compounds that included the desired unsymmetrically functionalized molecule. NMR analysis of this mixture, however, revealed that the double-bond configuration was scrambled during the NaN_3 reaction. This mixture was subjected to azide-reducing conditions, followed by tBoc protection of the resulting amino group. At this point, intermediate **3** and its *Z*-isomer were readily separated and purified via chromatography. The tBoc group was then removed from each alkene, independently, and the amino group was acylated with isobutyryl chloride. These dithianes were converted to the corresponding dimethyl acetals, **4** and its *Z*-isomer. The alkene configurations of the isomeric acetals were established by both NOE data (summarized in the Experimental Section) and IR data (**4** showed no sign of intramolecular N–H...OCH₃ hydrogen bonding, while the isomer displayed intramolecular hydrogen bonding, in dilute CH_2Cl_2 solution). Conversion of **4** to diamide **2** involved standard methods.

Intermediate **3** was used to prepare a wide variety of other molecules containing the ADPA unit, including tri- and tetrapeptide analogues, e.g., **11**. These syntheses involved standard methods for the most part; details are provided in the Supporting Information. Two of the molecules required for our studies, **16** and **17** (analogues of **11**), had an ester group in place of one secondary amide group. For **16**, synthesis involved use of the α -hydroxy analogue of L-leucine, which is readily available from

(12) Replacement of an ethylene unit with an alkene unit leads to little rigidification because of the low barrier to rotation about sp^2 – sp^3 bonds: Page, M. I.; Jencks, W. P. *Proc. Natl. Acad. Sci. U.S.A.* **1971**, *68*, 1678. Expansion of this concept: Mammen, M.; Shakhnovich, E. I.; Whitesides, G. M. *J. Org. Chem.* **1998**, *63*, 3168.

(13) We have previously shown that tri- and tetrasubstituted *trans*-alkene units provide greater backbone preorganization than a disubstituted *trans*-alkene unit, as manifested in intramolecular hydrogen bond formation: (a) Liang, G.-B.; Dado, G. P.; Gellman, S. H. *J. Am. Chem. Soc.* **1991**, *113*, 3994. (b) Liang, G.-B.; Desper, J. M.; Gellman, S. H. *J. Am. Chem. Soc.* **1993**, *115*, 925.

(14) Computational prediction that a *trans*-trisubstituted alkene-based amide isostere will more strongly induce chain folding than a *trans*-disubstituted alkene: Deschrijver, P.; Tourwé, D. *FEBS Lett.* **1982**, *146*, 353. Recent experimental efforts to verify this prediction were unsuccessful: Devadder, S.; Verheyden, P.; Jaspers, H. C. M.; Van Binst, G.; Tourwé, D. *Tetrahedron Lett.* **1996**, *37*, 703.

(15) (a) Murray, R. W.; Agarwal, S. K. *J. Org. Chem.* **1985**, *50*, 4698. (b) Gordon, B.; Blumenthal, M.; Mera, A. E.; Kumpf, R. J. *J. Org. Chem.* **1985**, *50*, 1540.

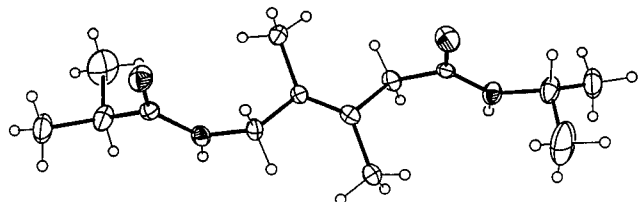


Figure 1. Conformation of **2** in the solid state.

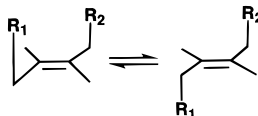


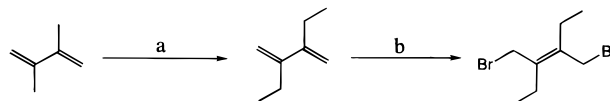
Figure 2. Influence of avoided allylic strain on the position of substituents R_1 and R_2 relative to the alkene plane.

L-leucine. Synthesis of **17** was accomplished by treating (*E*)-1,4-dibromo-2,3-dimethyl-2-butene with 1 equiv of 2-lithio-1,3-dithiane followed by CsOAc (rather than NaN_3) and then proceeding as described in the Supporting Information.

The alkene configuration of **2** was confirmed by X-ray crystallography (Figure 1). Interestingly, the molecule crystallized in an extended conformation, even though it was designed to adopt a folded conformation in solution (this folded conformation is highly populated in methylene chloride solution, as demonstrated below). For **2** and related molecules, avoidance of allylic strain is expected to keep the carboxyl and amino functional groups out of the alkene plane, but these groups can either reside on the same side of the alkene plane (desired; expected to promote β -hairpin folding) or on the opposite side (undesired; precludes β -hairpin folding). These two possibilities are illustrated in Figure 2. In the solid state, the undesired arrangement is displayed by **2** (Figure 1) and by four other molecules derived from **1** (including **17**).¹⁷ (The observation that **2** adopts an extended conformation in the solid state shows how profoundly intermolecular interactions in a crystal lattice can perturb the intrinsic conformational preferences of flexible molecules.¹⁶) Wipf et al. have recently reported crystal structures of two optically active alanylalanine dipeptide mimics related to **2** in which the alkene is trisubstituted, and a β -turn-like conformation is observed in both cases.^{4e}

It seemed possible that greater conformational preorganization might be achieved by replacing the vinyl methyl groups of amino acid **1** with larger groups, since avoidance of 1,5-*syn*-pentane-like interactions could induce the diagonal substituents (i.e., the carbonyl and nitrogen functional groups) to reside on the same side of the alkene. This type of conformation has been observed for tetrabenzylethylene in the solid state.¹⁸ We tested this hypothesis by examining diamide **5**, the diethyl analogue of **2**. Synthesis of **5** proceeded from (*E*)-2,3-dibromomethyl-3-hexene via the route described above for preparation of **2** from (*E*)-1,4-dibromo-2,3-dimethyl-2-butane. (*E*)-2,3-Dibromomethyl-3-hexene was prepared by converting 2,3-dimethylbutadiene to 2,3-diethylbutadiene,^{15b} followed by bromination^{15a} (Scheme 2). The alkene configuration of **5** was verified crystallographically.¹⁷ In the solid state, **5** displays an

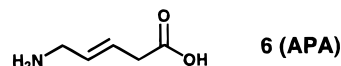
Scheme 2^a



^a Key: (a) KO^tBu , *n*-BuLi; MeI. (b) Br_2 .

extended conformation very similar to that seen for **2** (Figure 1), with all hydrogen bonding intermolecular. This observation is contradictory to our hypothesis but consistent with the results presented below that show the folding of **2** and **5** to be very similar in solution.

To evaluate our hypothesis that avoidance of allylic strain would provide useful conformational preorganization to a peptide chimera containing dipeptide mimic **1**, we required analogues containing the glycylglycine mimic *trans*-5-amino-pent-3-enoic acid (APA, **6**). Scheme 3 outlines preparation of



diamide **8**, which is an analogue of **2**. Intermediate **7** was useful for preparing other derivatives that are discussed below.

Solvent Choice. All molecules were examined in methylene chloride solution. The di-, tri-, and tetrapeptide analogues we prepared are not expected to fold extensively in a highly polar solvent, like water, because there is insufficient noncovalent driving force for adoption of a compact conformation. Indeed, conventional peptides comprised of two to four residues do not generally display significant populations of folded conformers in aqueous solution. By working in a relatively nonpolar solvent, we allow intramolecular hydrogen bonds to serve as a driving force for folding. Hydrogen bond formation also provides a sensitive method for detecting folding conformations and identifying the folding pattern under these conditions.

Extensive reports from our lab^{8a,b,13,19} and others²⁰ demonstrate that formation of one or two amide–amide hydrogen bonds provides a significant but not overwhelming inducement for folding in solvents such as methylene chloride and chloroform. This situation is ideal for examining the intrinsic folding propensity of the covalent structure that links the hydrogen-bonding sites, particularly if the analysis involves comparing molecules that could form identical numbers and types of hydrogen bonds (e.g., comparison of dipeptide mimics **2**, **5**, and **8**). The intrinsic folding propensity is determined by several factors, including torsional strain and other nonbonded repulsions that develop as the backbone folds back upon itself, and the conformational entropy loss that accompanies folding. Since solvation forces are expected to exert relatively little influence on the intrinsic folding propensity, the insights gained from analysis in organic solvents should apply to aqueous solution as well. Indeed, we have established such a correlation in our analysis of the stereochemical requirements for formation of β -hairpins with two-residue loops.^{9a–e} We initially used tetrapeptides and related compounds, examined in methylene chloride, to demonstrate that placing D-proline at the first of the two loop residues strongly promotes β -hairpin folding, relative to L-proline at the same position.^{9a,b} Subsequently, we

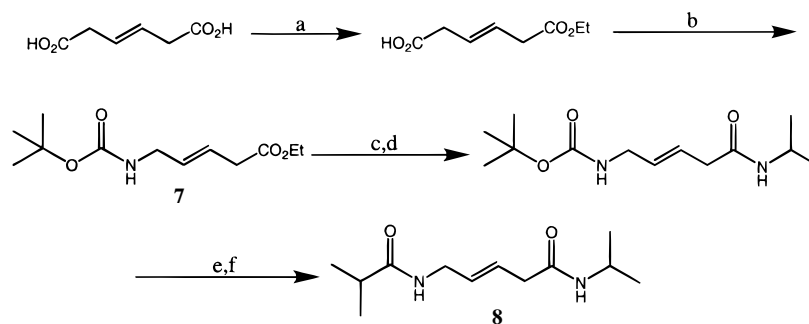
(19) (a) Gellman, S. H.; Dado, G. P.; Liang, G.-B.; Adams, B. R. *J. Am. Chem. Soc.* **1991**, *113*, 1164. (b) Liang, G.-B.; Desper, J. M.; Gellman, S. H. *J. Am. Chem. Soc.* **1993**, *115*, 925.

(20) For leading references, see: (a) Tsang, K. Y.; Diaz, H.; Graciani, N.; Kelly, J. W. *J. Am. Chem. Soc.* **1994**, *116*, 3988. (b) Nowick, J. S.; Abdi, M.; Bellamo, K. A.; Love, J. A.; Martinez, E. J.; Noronha, G.; Smith, E. M.; Ziller, J. W. *J. Am. Chem. Soc.* **1995**, *117*, 89. (c) Gung, B. W.; Zhu, Z. *J. Org. Chem.* **1996**, *61*, 6482.

(16) For previous examples of the effects of crystal lattices on the conformations of flexible, polar molecules, see: (a) Dado, G. P.; Desper, J. M.; Holmgren, S. K.; Rito, C. J.; Gellman, S. H. *J. Am. Chem. Soc.* **1992**, *114*, 4834. (b) Gellman, S. H.; Powell, D. R.; Desper, J. M. *Tetrahedron Lett.* **1992**, *33*, 1963. (c) Kessler, H.; Zimmermann, G.; Förster, H.; Engel, J.; Oepen, G.; Sheldrick, W. S. *Angew. Chem., Int. Ed. Engl.* **1981**, *20*, 1053.

(17) Gardner, R. R., Ph.D. Thesis, University of Wisconsin—Madison, 1997.

(18) Andersen, L.; Berg, U.; Pettersson, I. *J. Org. Chem.* **1985**, *50*, 493.

Scheme 3^a

^a Key: (a) (Ethanol, H₂SO₄ (cat.)). (b) (PhO)₂P(O)N₃, *tert*-butanol, reflux. (c) NaOH, ethanol, H₂O. (d) DCC, *N*-hydroxysuccinimide, isopropylamine. (e) 4 N HCl, dioxane. (f) Isobutyryl chloride, Et₃N.

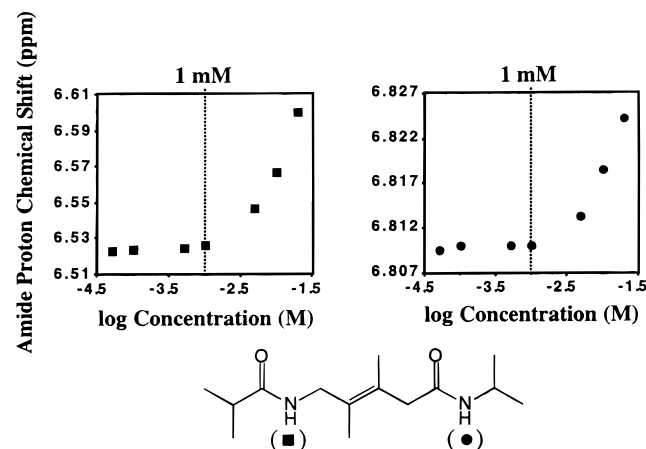


Figure 3. Amide proton NMR chemical shifts for **2** in CD₂Cl₂ at room temperature, as a function of the logarithm of concentration. These data suggest that aggregation occurs above 1 mM.

showed that analogous effects are manifested with 12–16 residue peptides in aqueous solution.^{9e–c}

Conformational Analysis of Dipeptide Mimics. Study of hydrogen-bond-driven folding processes in nonpolar solvents must begin with control experiments to determine the lowest concentration at which intermolecular hydrogen bonding occurs. Figure 3 shows how the amide proton chemical shifts of **2** vary as a function of the logarithm of concentration in CD₂Cl₂. These data suggest that intermolecular hydrogen bonding occurs only above 1 mM. The NMR and IR data discussed below were obtained at 1 mM and should reflect effects of only intramolecular hydrogen bonding, unless otherwise mentioned.

Figure 4 shows N–H stretch region IR data for dipeptide mimics **2**, **5**, and **8** and for reference compounds **9** and **10**, each 1 mM in CH₂Cl₂ at room temperature. There are at least four bands for **2** in this region, as shown by the mathematical decomposition of the spectral data. Extensive precedent^{13,19,21} indicates that the bands at 3453 and 3436 cm⁻¹ arise from N–H groups exposed to solvent, the band at 3330 cm⁻¹ arises from N–H involved in an intramolecular amide–amide hydrogen bond, and the band at 3410 cm⁻¹ arises from N–H involved in a weaker hydrogen bond. We assign the band at 3453 cm⁻¹ to the N-terminal N–H, which appears to be free of intramolecular hydrogen bonding. The other three bands are assigned to the C-terminal N–H. The most highly populated state of this N–H involves a 10-membered ring C=O–H–N hydrogen bond (the desired β -turn-like folding pattern); the two less populated states

proposed to be are solvent-exposed (3436 cm⁻¹) and an intramolecular N–H– π hydrogen-bonded form (3410 cm⁻¹), involving the alkene as acceptor.²² The ca. 17 cm⁻¹ difference between non-hydrogen-bonded N-terminal and C-terminal N–H stretch bands is consistent with prior observations that a branched alkyl group on nitrogen causes the N–H bands of secondary amides to move 15–20 cm⁻¹ to lower energy, relative to N–H bands of secondary amides with linear alkyl appendages.²¹

Our conclusion that **2** experiences extensive 10-membered ring but no eight-membered ring hydrogen bonding is supported by the data for reference compound **9**, in which only the eight-membered ring hydrogen bond is possible. This molecule displays a single N–H band, at 3440 cm⁻¹, in the region for solvent-exposed N–H. The difference between the positions of this band and the band assigned to the analogous solvent-exposed N–H in **2** (ca. 13 cm⁻¹) may indicate that there is a different torsional preference about the (O=)CN–CC(=C) bond between these two molecules.²³ This difference also indicates that great caution must be exercised in trying to interpret variations of <20 cm⁻¹ in N–H stretch band positions between different molecules.

Comparison of IR data for **2** with the data for **8**, the analogue containing a disubstituted alkene, confirms our prediction that the tetrasubstituted alkene strongly preorganizes the backbone for β -turn-like folding. Dipeptide **8** experiences much less intramolecular hydrogen bonding than does **2**. Further, the data for reference compound **10** indicate that intramolecular hydrogen bonding in the disubstituted alkene series arises in part or entirely from eight-membered ring formation. These results demonstrate that avoidance of allylic strain provides useful control of conformational preferences.

Comparison of IR data for **2** with the data for **5**, the analogue containing ethyl groups rather than methyl groups on the tetrasubstituted alkene, contradicts our hypothesis that avoidance of *syn*-pentane-like interactions would lead to enhanced conformational control. Diamides **2** and **5** display nearly identical extents of internal hydrogen bonding. It is possible that the desired level of conformational control could be achieved with substituents larger than ethyl on the alkene.

Conformational Analysis of Tetrapeptide Mimics. A large propensity to adopt a U-shape does not ensure that a molecular fragment will serve as a successful β -hairpin promoter.^{9a–d} We therefore evaluated the β -hairpin-promoting properties of the ADPA and APA glycyglycine mimics by placing them at the center of tetrapeptide analogues. Tetrapeptides can fold to

(21) (a) Boussard, G.; Marraud, M. *Biopolymers* **1979**, *18*, 1297. (b) Maxfield, F. R.; Leach, S. J.; Timson, E. R.; Powers, S. P.; Scheraga, H. A. *Biopolymers* **1979**, *18*, 2507.

(22) (a) Gallo, E. A.; Gellman, S. H. *Tetrahedron Lett.* **1992**, *33*, 7485. (b) Ref. 13b.

(23) Aaron, H. S. *Top. Stereochem.* **1980**, *11*, 1.

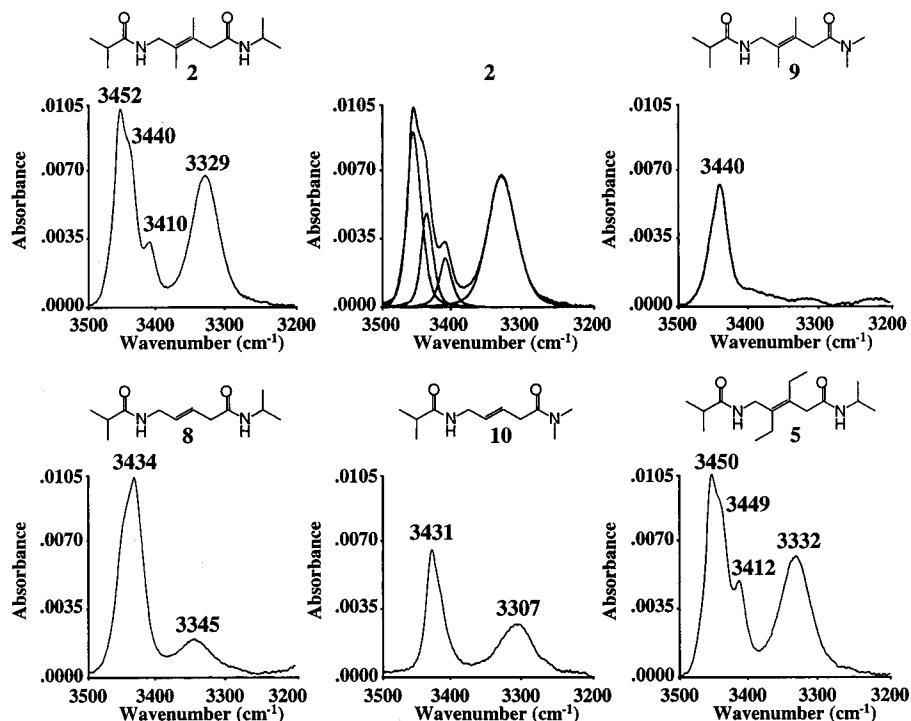


Figure 4. N–H stretch region FT-IR data for 1 mM samples of **2**, **5**, and **8–10** in CH_2Cl_2 at room temperature, after subtraction of the spectrum of pure CH_2Cl_2 . For **2**, the bands implied by curve fitting analysis are also shown.

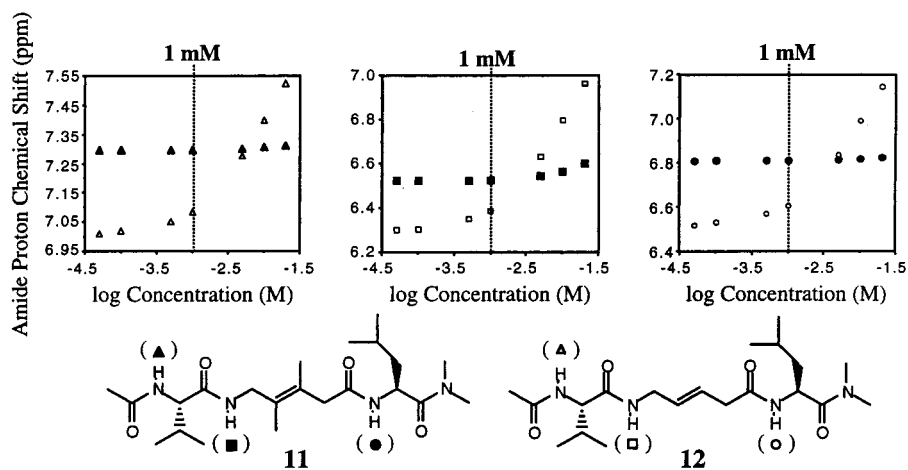


Figure 5. Amide proton NMR chemical shifts for **11** and **12** in CD_2Cl_2 at 20 °C, as a function of the logarithm of concentration.

minimal β -hairpins, in which the central two residues form the loop and each terminal residue constitutes a strand.^{9a,b} In such systems, two internal amide–amide hydrogen bonds are formed. The inner hydrogen bond (10-membered ring) corresponds to β -turn formation, and the outer hydrogen bond (14-membered ring) is a key criterion for β -hairpin formation.

Molecule **11** is a tetrapeptide analogue in which the ADPA glycyglycine mimic replaces the central two residues; if **11** adopted a β -hairpin-like folding pattern, the valine and leucine residues would constitute the strands. Tetrapeptide analogue **12** is based on the APA disubstituted alkene mimic. Figure 5 shows the variation of amide proton chemical shifts of **11** and **12** as a function of the logarithm of concentration. These data indicate that **12** is more prone to aggregation than is **11**. This difference provides indirect evidence that **11** is intramolecularly hydrogen bonded to a greater extent, and therefore less available for intermolecular hydrogen bonding, than is **12**.

Insight on the internal hydrogen-bonding patterns experienced by **11** and **12** in methylene chloride is available from the amide

proton chemical shifts at low concentrations, along with analogous data from reference compounds **13–15** (Figure 6). Equilibration among internally hydrogen-bonded and non-hydrogen-bonded states of small molecules is generally rapid on the NMR time scale. An amide proton involved in such equilibration gives rise to a single resonance, which is a population-weighted average of the contributing hydrogen-bonded and non-hydrogen-bonded states. Hydrogen-bonded forms are generally downfield of non-hydrogen-bonded forms. Because of differences in spectroscopic time scales, hydrogen-bonding information from NMR chemical shifts is complementary to information provided by IR data. Equilibration between hydrogen-bonded and non-hydrogen-bonded states is slow on the IR time scale; therefore, hydrogen-bonded and non-hydrogen-bonded states of a given N–H group give rise to distinct bands in the IR spectrum (cf. Figure 4).

The data in Figure 6 indicate extensive folding of tetrapeptide mimic **11** in CD_2Cl_2 solution. Each of the two NH chemical shifts observed for reference compound **13** is nearly identical

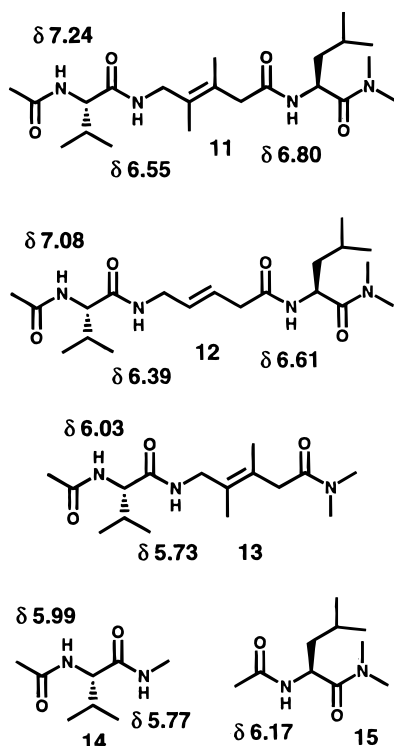


Figure 6. Structures of **11**–**15**, with NH chemical shifts measured at 1 mM in CD₂Cl₂.

to the analogous NH chemical shift for reference compound **14**, which shows that the carbonyl of the dipeptide mimetic unit does not form hydrogen bonds to the N-terminal residue. Thus, neither 8- nor 11-membered ring hydrogen bonding is expected in tetrapeptide mimic **11**. (The absence of eight-membered ring hydrogen bonding in **13** is consistent with our findings for **9**, discussed above.) Relative to the appropriate NH of reference compounds **13** and **14**, the N-terminal NH of **11** is shifted downfield by 1.2 ppm, which suggests that this NH is involved in considerable intramolecular hydrogen bonding. These results imply that the acceptor is the leucine C=O (14-membered ring hydrogen bond), and this end-to-end interaction suggests that the desired β -hairpin-like folding pattern (**I**, Figure 7) is significantly populated.

One surprising feature of the chemical shift data in Figure 6 is the 0.8 ppm downfield shift of the central NH of **11** relative to the analogous NHs of **13** and **14**. In the β -hairpin-like folding pattern (**I**, Figure 7), this central NH is exposed to solvent, but the downfield shift in **11** relative to **13** and **14** suggests that this NH participates in intramolecular hydrogen bonding with the C-terminal (leucine) carbonyl (11-membered ring hydrogen bond). Since this hydrogen bond cannot occur in the β -hairpin-like conformation, we propose that **11** equilibrates between the β -hairpin-like folding pattern and at least one other folded conformation. This additional folded state could involve only the 11-membered ring hydrogen bond to the C-terminal carbonyl (**II**, Figure 7), or simultaneous 11- and 14-membered ring hydrogen bonds to this carbonyl (**III**, Figure 7). An N–H $\cdots \pi$ interaction could occur between the leucine NH and the alkene in the additional folded state (shown in both **II** and **III**, Figure 7).

NH chemical shift data for **12** at 1 mM in CD₂Cl₂ (Figure 6) suggest that intramolecular hydrogen bonding is diminished, relative to **11**, because all NH resonances of **12** are upfield of the analogous NH resonances of **11**. The data in Figure 5 show that **12** experiences some aggregation at 1 mM, which means

that the chemical shifts reported for **12** in Figure 6 are downfield-shifted relative to the true “monomeric” values. The differences between **11** and **12** in Figure 6 support our conclusion that the tetrasubstituted alkene unit more effectively promotes β -hairpin-like folding than does the disubstituted alkene unit.

Comparison of N–H stretch region IR data for tetrapeptide mimics **11** and **12** (Figure 8; 1 mM in CH₂Cl₂) indicates that there is a greater extent of intramolecular hydrogen bonding in **11** than in **12**, which is consistent with a greater folding propensity for **11**. Bands above 3400 cm⁻¹ arise largely from solvent-exposed N–H groups, while bands below 3400 cm⁻¹ arise from hydrogen-bonded N–H groups. Although each tetrapeptide mimic displays a complex spectrum in this region, the larger amount of C=O \cdots H–N hydrogen bonding in **11** is readily apparent from the dominant band at 3326 cm⁻¹. IR data for reference compounds **13**–**15** reveal no bands below 3420 cm⁻¹; thus, the N–H groups in these molecules are solvent exposed or engaged in “C₅ interactions”. (The term C₅ designates C=O \cdots H–N interactions within a single residue; whether this five-membered ring interaction constitutes a weak hydrogen bond has been a subject of debate because of the necessarily poor geometry (O–H–N angle < 100°).) The absence of conventional C=O \cdots H–N hydrogen bonding within **13**–**15** indicated by the IR data is consistent with the conclusions drawn above from the NMR data in Figure 6, i.e., that internal hydrogen bonding in **11** results from folding patterns **I** plus **II** and/or **III**.

We used ¹⁵N-labeling to gain further information from N–H stretch IR spectroscopy of **11**. The stretch band of a ¹⁵N–H unit is expected to occur ca. 12 cm⁻¹ lower than the stretch band of the analogous ¹⁴N–H unit.²⁵ We have previously shown that site-specific incorporation of ¹⁵N into molecules with multiple secondary amide groups can facilitate assignment of N–H stretch bands.²⁶ Figure 9 shows N–H stretch region IR data for **11** without labels, and for two labeled versions, one with ¹⁵N at the leucine N–H (**11**-¹⁵N-Leu) and one with ¹⁵N at the valine NH (**11**-¹⁵N-Val). Also shown in Figure 9 is a deconvolution of each spectrum into five component bands. Assignments of the five N–H stretch bands identified for **11** can be made, based on the effects of labeling two of the three secondary amide groups with ¹⁵N. We present these assignments for **11** by considering each NH group individually.

The valine NH contributes to the 3421 and 3288 cm⁻¹ bands identified for **11** because the former shifts to 3415 cm⁻¹ and the latter to 3280 cm⁻¹ in **11**-¹⁵N-Val, while the other three bands are not significantly shifted in this compound. The band at 3288 cm⁻¹ arises from a strong amide–amide hydrogen bond; we assign this band to valine NH involved in the 14-membered ring hydrogen bond of β -hairpin-like conformation **I** (Figure 7). The band at 3421 cm⁻¹ is assigned to valine NH involved in a C₅ interaction, which is consistent with conformation **II**, but not with the bifurcated interaction of conformation **III**.

(24) (a) Avignon, M.; Huong, P. V.; Lascombe, J.; Marraud, M.; Neel, J. *Biopolymers* **1969**, *8*, 69. (b) Burgess, A. W.; Scheraga, H. A. *Biopolymers* **1973**, *12*, 2177.

(25) For a localized A–B stretch, the band position can be estimated from the equation $\nu = (2\pi c)^{-1}[k(M_A + M_B)/M_A M_B]^{1/2}$

where c is the speed of light, k is the force constant of the A–B bond, M_A is the mass of atom A, and M_B is the mass of atom B. (Silverstein, R. M.; Bassler, G. C.; Morrill, T. C. *Spectrometric Identification of Organic Compounds*, 5th ed.; John Wiley & Sons: New York, 1991; p 93). This calculation predicts a localized ¹⁵N–H stretch to be ca. 12 cm⁻¹ lower in energy than a ¹⁴N–H stretch.

(26) (a) Gallo, E. A.; Gellman, S. H. *J. Am. Chem. Soc.* **1993**, *115*, 9774. (b) Gardner, R. R.; Gellman, S. H. *J. Am. Chem. Soc.* **1995**, *117*, 10411.

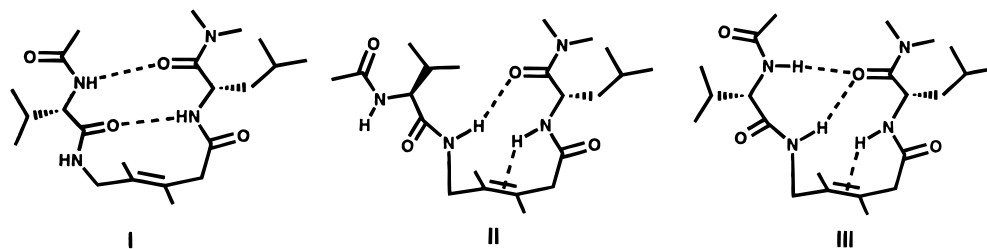


Figure 7. Alternative folding patterns for tetrapeptide mimic **11** (see text for details).

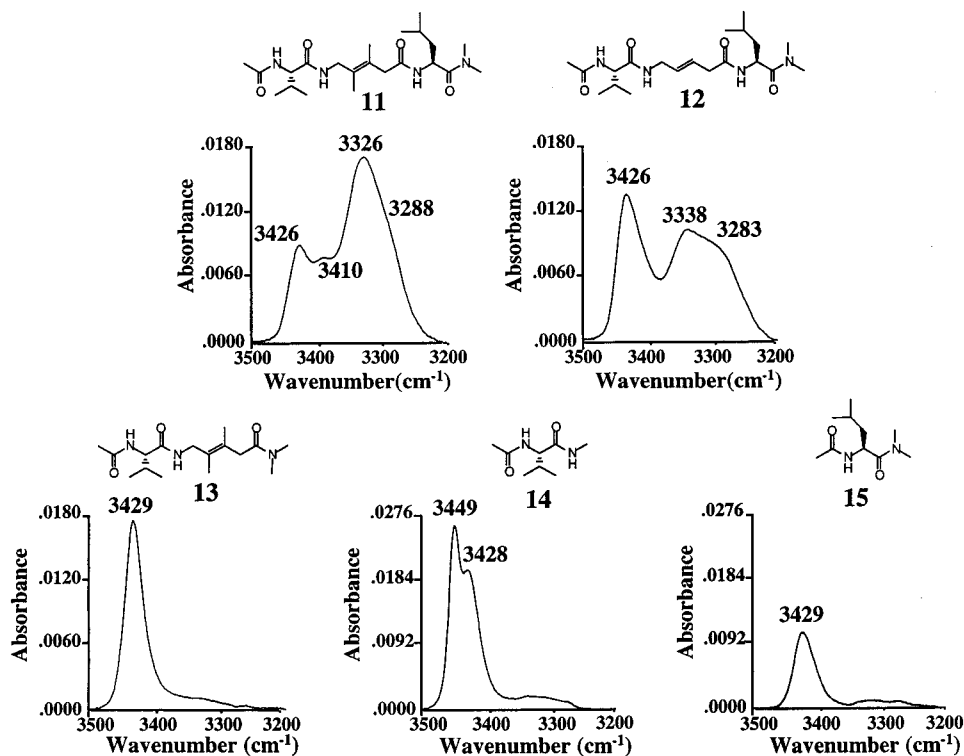


Figure 8. N–H stretch region FT-IR data for 1 mM samples of **11**–**15** in CH₂Cl₂ at room temperature, after subtraction of the spectrum of pure CH₂Cl₂.

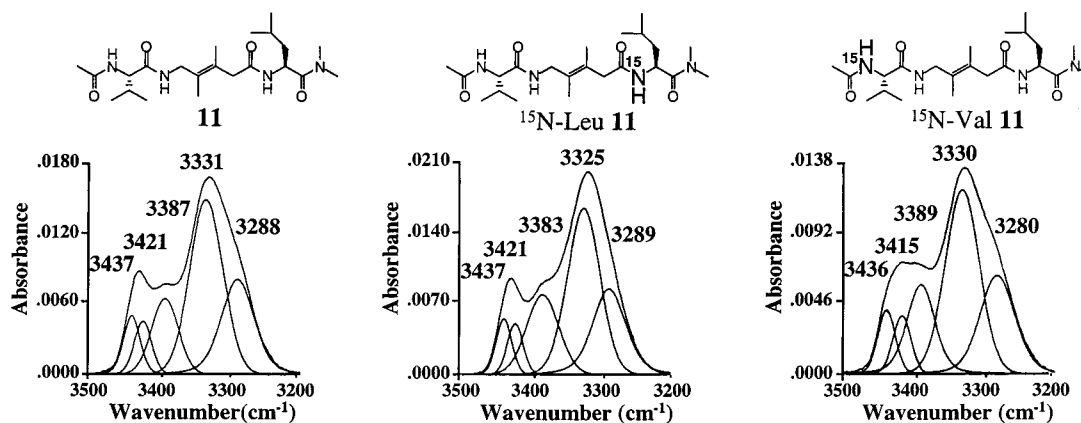


Figure 9. N–H stretch region FT-IR data for 1 mM samples of **11** and two ¹⁵N-labeled versions in CH₂Cl₂ at room temperature, after subtraction of the spectrum of pure CH₂Cl₂. The bands implied by curve fitting analysis are also shown.

The leucine NH contributes to the 3387 and 3331 cm⁻¹ bands identified for **11** because the former shifts to 3383 cm⁻¹ and the latter to 3325 cm⁻¹ in **11**-¹⁵N-Leu, while the other three bands are not significantly shifted. The large band at 3325 cm⁻¹ represents NH involved in an amide–amide hydrogen bond, and we assign this band to the 10-membered ring hydrogen bond of β -hairpin-like conformation **I**; as discussed below, we suspect that there is also another hydrogen-bonded NH contribution to the large 3325 cm⁻¹ band. The band at 3387 cm⁻¹ is assigned

to leucine NH involved with the alkene in an N–H- π hydrogen bond. This band is 23 cm⁻¹ lower than the band assigned to the N–H- π interaction in **2**; we have no explanation for this difference. The proposed N–H- π interaction in **11** is consistent with conformation **II** or **III**.

The internal NH of **11** (i.e., the NH of the ADPA glycylglycine mimic) was not ¹⁵N-labeled because of the synthetic difficulty of this task. Nevertheless, the band at 3437 cm⁻¹ can be assigned to this internal NH, since this band does not shift

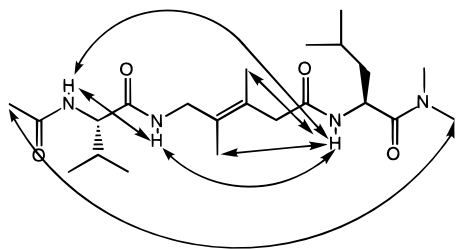


Figure 10. Summary of nonadjacent NOEs detected for **11** in CD_2Cl_2 .

in either ^{15}N -labeled molecule. This band position indicates a solvent-exposed NH (cf. IR data for reference compound **9**), as expected for β -hairpin-like folding pattern **I** (Figure 7). Since the 3437 cm^{-1} band is relatively small, it is likely that the internal NH of **11** contributes to at least one other band in the spectrum. We propose that the internal NH contributes to the large band at 3331 cm^{-1} , which would imply that this NH is involved in a strong amide–amide hydrogen bond, as required for conformation **II** or **III**.

The ^{15}N -labeling/deconvolution studies provide support for our conclusion that **11** adopts β -hairpin-like folding pattern **I**. These studies also support our deduction that **11** adopts a second folded conformation, most likely **II**, in which the leucine NH is involved in an N–H- π interaction with the alkene, the valine NH is exposed to solvent or engaged in a C_5 interaction, and the internal NH forms an 11-membered ring hydrogen bond with the leucine carbonyl.

NOESY²⁷ studies were carried out with tetrapeptide mimic **11** to gain additional understanding of the folded conformations adopted by this molecule in methylene chloride solution. The long-range NOEs observed in a 1 mM solution are summarized in Figure 10. None of the conformations shown in Figure 7, alone, can account for all of these long-range NOEs; therefore, the NOESY data provide further evidence of multiple folded conformations. The NOE between valine NH and leucine NH can be explained only by the β -hairpin-like folding pattern (**I**, Figure 7). The NOEs between leucine NH and the two alkene methyl groups, and between the terminal methyl groups, are consistent with the β -hairpin-like folding pattern but could also be explained in other ways: the leucine NH-alkene methyl NOEs could arise from conformation **II** or **III**, and the NOE between the terminal methyl groups could arise from **III** (but not **II**). The NOEs between valine NH and the internal NH, and between the internal NH and leucine NH, cannot arise from β -hairpin-like conformation **I**; the former is consistent with conformation **III**, and the former, with **II** or **III**.

Further information on the folding behavior of **11** was obtained by examination of two analogues, **16** and **17**, in which one secondary amide group is replaced by an ester group. As we have previously pointed out, this replacement is conservative in the sense that the secondary amide and ester groups have similar conformational preferences.²⁶ However, ester and secondary amide groups differ profoundly in their hydrogen-bonding properties, since the ester cannot donate a hydrogen bond and the ester is a much weaker acceptor than the amide.²⁸ Figure 11 summarizes amide proton chemical shifts of **16** and **17** (1 mM in CD_2Cl_2), for comparison with Figure 5. Figure 12 shows N–H stretch region IR data for **16** and **17**.

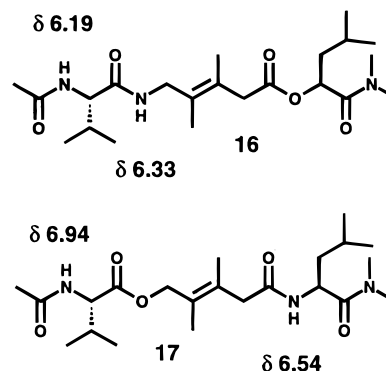


Figure 11. Structures of **16** and **17**, with NH chemical shifts measured at 1 mM in CD_2Cl_2 .

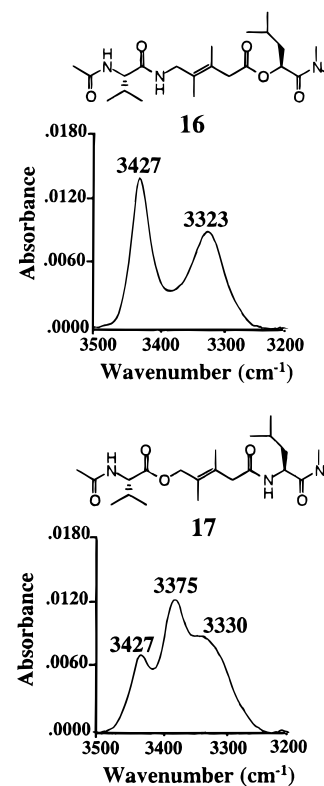


Figure 12. N–H stretch region FT-IR data for 1 mM samples of **16** and **17** in CH_2Cl_2 at room temperature, after subtraction of the spectrum of pure CH_2Cl_2 .

In **16**, the leucine NH is replaced by an ester oxygen; this molecule allows us to test the favorability of proposed folding patterns **II** and **III** in Figure 7. A β -hairpin-like folding pattern, analogous to **I**, should be strongly disfavored in **16**, since the ester placement precludes formation of the “inner” 10-membered ring hydrogen bond. On the other hand, the favorability of the folding pattern analogous to **II** should not be compromised in **16** relative to **11**. Although the N–H- π hydrogen bond shown in Figure 7 for **II** and **III** cannot form in **16**, it is unlikely that this weak interaction would be a dominant contributor to conformational stability.

The behavior of **16** indicates that folding patterns such as **II**, and perhaps **III**, are reasonable conformations for this class of tetrapeptide analogues, but that neither **II** nor **III** can be the major conformation adopted by **11**. Comparison of the amide proton chemical shifts for **16** (Figure 11) and reference compound **12** (Figure 6) suggests that there is significant 11-membered ring hydrogen bonding in **16**, between the C-terminal

(27) Macura, S.; Ernst, R. R. *Mol. Phys.* **1980**, *41*, 95.

(28) (a) Arnett, E. M.; Mitchell, E. J.; Murty, T. S. S. R. *J. Am. Chem. Soc.* **1974**, *96*, 3875. (b) Spencer, J. N.; Garrett, R. C.; Moyer, F. J.; Merkle, J. E.; Powell, C. R.; Tran, M. T.; Berger, S. K. *Can. J. Chem.* **1980**, *58*, 1372.

amide carbonyl and the NH of the dipeptide mimic because this δNH in **16** is 0.6 ppm downfield relative to **13**. In contrast, the valine NH resonances are less than 0.2 ppm apart in **16** and **13**, which suggests that a folding pattern like **II** is preferable to a folding pattern like **III**. The N–H stretch region IR data for **16** (Figure 12) confirm that this molecule experiences significant intramolecular hydrogen bonding (3323 cm^{-1}); however, most of the N–H groups of **16** are solvent-exposed or engaged in a C_5 interaction because the 3427 cm^{-1} band is larger than the 3323 cm^{-1} band (hydrogen-bonded bands have larger extinction coefficients than non-hydrogen-bonded bands²⁹). Comparison of the IR data for **16** with the IR data for **11** (Figure 8) shows that there is considerably less intramolecular hydrogen bonding in **16** than in **11**. Thus, there must be another major intramolecularly hydrogen-bonding pattern available to **11**, presumably β -hairpin-like conformation **I**.

In **17**, the NH of the dipeptide mimic unit is replaced with an ester oxygen. In this case, it is impossible to have the 11-membered ring hydrogen bond central to folding patterns **II** and **III** (Figure 7), but a β -hairpin-like folding pattern, analogous to **I** can form, with the ester serving as the acceptor for the “inner” 10-membered ring hydrogen bond. Both NMR and IR data suggest that there is considerable β -hairpin-like folding of **17**, even though the ester–amide hydrogen bond is weaker than the corresponding amide–amide hydrogen bond of **11**.^{26,28} The valine δNH is quite far downfield (Figure 11; compare analogous δNH of **13** and **11**, in Figure 6), which is consistent with substantial 14-membered ring hydrogen bonding. The leucine δNH of **17** is also downfield shifted, relative to reference compound **15**; since esters are weaker acceptors than amides,^{26,28} the maximum downfield shift for leucine δNH in **16** is probably smaller than the fully hydrogen bonded limit of the leucine δNH in **11**. IR data (Figure 12) show that **17** is intramolecularly hydrogen bonded to a large extent. Only a relatively small band (3427 cm^{-1}) is observed in the solvent-exposed/ C_5 region. The large band at 3375 cm^{-1} is assigned to the ester–amide hydrogen bond (10-membered ring) of the β -hairpin-like folding pattern, and the shoulder at 3330 cm^{-1} is assigned to the amide–amide hydrogen bond (14-membered ring).

Conclusion. Our analysis of di-, tri-, and tetrapeptide analogues containing the ADPA glycyglycine mimic demonstrates that avoidance of allylic strain within a tetrasubstituted alkene unit provides significant conformational preorganization. Use of the tetrasubstituted (*E*)-alkene favors adoption of folded conformations more strongly than does the more conventional APA disubstituted alkene “amide isostere.” The desired β -hairpin-like folding pattern is adopted when the ADPA glycyglycine mimic is placed at the center of a tetrapeptide analogue (**11**); however, at least one other folding pattern is also populated in this case, in methylene chloride solution. Our analysis shows how a combination of NMR and IR techniques, along with careful choice of reference compounds, can elucidate a conformational equilibrium involving multiple intramolecularly hydrogen bonded states. These results suggest that the ADPA glycyglycine mimic may be useful for pharmaceutical and molecular design applications.

Experimental Section

General Procedure. All melting points are uncorrected. Reagents employed were either commercially available or prepared according to a known procedure. Anhydrous CH_2Cl_2 and *t*-BuOH were obtained by distillation from CaH_2 . All other solvents used were reagent grade

except for hexane, which was purified by distillation. Anhydrous reaction conditions were maintained under a slightly positive nitrogen atmosphere in oven-dried glassware. Silica gel chromatography was performed using 230–400 mesh silica purchased from EM Science. Routine ^1H and ^{13}C NMR spectra were obtained on a Bruker AM-300 spectrometer at 300.132 and 75.033 MHz frequencies, respectively. NMR spectra were referenced to tetramethylsilane (TMS) (0 ppm) or to the isotopic impurity peak of CDCl_3 (7.26 and 77.0 ppm for ^1H and ^{13}C , respectively). Routine infrared spectra were obtained using a Nicolet 740 FT-infrared spectrometer. High-resolution electron impact ionization mass spectroscopy was performed using a Kratos MS-25 spectrometer.

IR Studies. High-quality infrared spectra (128 scans) were obtained at 2 cm^{-1} resolution using a 1 mm CaF_2 solution cell and a Nicolet 740 FT-infrared spectrometer. All spectra were obtained in 1 mM solutions in anhydrous CH_2Cl_2 at 297 K. All compounds that were studied were judged to be >95% pure by examination of 500 MHz ^1H NMR spectra. All compounds were dried in vacuo at elevated temperatures in the presence of P_2O_5 . CH_2Cl_2 was distilled from CaH_2 and stored over activated 4 Å molecular sieves. All sample preparations were performed in a nitrogen atmosphere.

^1H NMR Studies. ^1H NMR spectra for the concentration-dependence studies were obtained using a Bruker AM-500 spectrometer. Compounds were dried in vacuo at elevated temperatures in the presence of P_2O_5 . CD_2Cl_2 was dried by being stored over activated 4 Å molecular sieves for a minimum of 4 days. All sample preparations were performed in a nitrogen atmosphere. Solutions for temperature-dependence studies were 1 mM in CD_2Cl_2 and were degassed and placed in sealed NMR tubes. All spectra were referenced relative to the isotopic impurity peak in CD_2Cl_2 , which was assumed to be 5.320 at all temperatures.

Samples for two-dimensional ^1H NMR experiments were prepared as described above. All two-dimensional NMR spectra were obtained on a Varian Unity-500 spectrometer at 298 K. Proton signals were assigned from TOCSY³⁰ and NOESY²⁷ spectra. Two-dimensional spectra were obtained using standard Varian pulse sequences, and the data were processed with Varian V-NMR version 4.3 software. TOCSY spectra were recorded with 2048 data points in t_1 , 256 data points in t_2 , 16 scans per t_2 increment, sweep width = 4000 Hz, relaxation delay = 600 ms, and a mixing time of 60 ms. NOESY spectra were recorded with 2048 data points in t_1 , 512 data points in t_2 , 128 scans per t_2 increment, sweep width = 4000 Hz, relaxation delay = 2500 ms, and a mixing time of 900 ms. (This mixing time was well below the T_1 measured for the amide NH resonances and most other resonances in the molecule.)

Synthesis. Preparative routes for diamides **2** and **5** are provided below. Additional synthetic protocols may be found in the Supporting Information.

***N*-(*tert*-Butoxycarbonyl)-2,3-dimethyl-4-(2,6-dithianyl)-(*E*)-2-butynamine (**3**).** A solution of 1,3-dithiane (7.08 g, 59 mmol) in anhydrous tetrahydrofuran (THF) (130 mL) was cooled to $-30\text{ }^\circ\text{C}$ under N_2 . A solution of *n*-butyllithium (22.5 mL, 2.6 M in hexane, 59 mmol) was added dropwise over 40 min. After being stirred for an additional 80 min, the solution was added dropwise (via a cannula) over 2 h to a solution of 1,4-dibromo-2,3-dimethyl-3-(*E*)-butene (14.4 g, 59.5 mmol) in anhydrous THF (100 mL) at $-78\text{ }^\circ\text{C}$. The resulting yellow solution was stirred for 6 h while being warmed to room temperature. The reaction mixture was quenched with water (50 mL) and then concentrated to a total volume of 100 mL. The organic layer was separated, and the aqueous layer was extracted with Et_2O ($2 \times 60\text{ mL}$). The combined organic layers were concentrated in vacuo, and the semisolid residue was taken up in water (50 mL). This mixture was treated with NaN_3 (4.36 g, 67 mmol) and Bu_4NBr (1.9 g, 5.9 mmol), and the two-phase mixture was stirred at $80\text{ }^\circ\text{C}$ for 10 h. The reaction mixture was cooled, and the organic phase was separated. The aqueous layer was extracted with Et_2O (50 mL), and the combined organic layers were concentrated to yield a brown viscous liquid. This material was taken up in THF (170 mL) and water (30 mL) and then was treated

(29) Pimentel, G. C.; McClellan, A. L. *The Hydrogen Bond*; Freeman: San Francisco, CA, 1960.

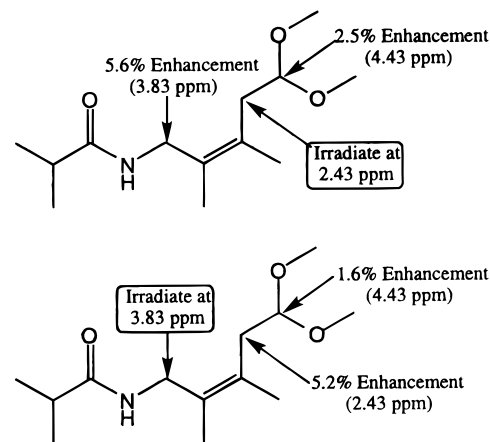
(30) Bax, A.; Davis, D. G. *J. Magn. Reson.* **1985**, *65*, 355.

with triphenylphosphine (23.2 g, 88.5 mmol) and stirred at room temperature for 30 h. The THF was removed in vacuo, and the resulting material was mixed with CHCl_3 . This solution was extracted with 1 N HCl (4 \times 50 mL). The combined acid extracts were carefully treated with 10 N NaOH until the pH of the solution was greater than 10, which caused formation of a dark layer at the top of the mixture. The two-phase mixture was extracted with Et_2O (5 \times 50 mL), and the combined organic layers were dried with Na_2SO_4 and concentrated to give the desired amine (4.32 g) as a mixture of isomers. ^1H NMR (CDCl_3/TMS , ppm): 1.50 (broad, 2H, NH), 1.7–1.8 (m, 6H, 4 \times CH_3), 1.8–2.3 (m, 2H, 2 \times CH_2), 2.48 (d, J = 7.90 Hz, 2H, CH_2), 2.53 (d, J = 8.30 Hz, 2H, CH_2), 2.8–2.9 (m, 4H, 4 \times SCH_2), 3.27 (s, 2H, NCH_2), 3.28 (s, 2H, NCH_2), 4.18 (t, J = 7.90 Hz, 1H, SCH_2), 4.22 (t, J = 8.30 Hz, 1H, SCH_2). The *E/Z* isomer ratio was \sim 1:1. A solution of the crude isomeric mixture of amines (1.0 g, 4.6 mmol) in dioxane (10 mL) and water (5 mL) was treated with potassium carbonate (0.73 g, 5.3 mmol) and di-*tert*-butyl dicarbonate (1.1 g, 5.06 mmol). This mixture was stirred at 0 $^\circ\text{C}$ for 3 h. The dioxane and water were removed in vacuo, yielding a dark oil that was purified by silica gel chromatography eluting with 15% (v/v) EtOAc in hexanes. The second isomer to elute was the desired *E*-isomer (**3**) as a white solid (0.74 g, 17.5%). Mp: 52.0–55.0 $^\circ\text{C}$. ^1H NMR (CDCl_3/TMS , ppm): 1.45 (s, 9H, CH_3), 1.75, 1.77 (2 \times m, 6H, CH_3), 1.8–2.2 (m, 1H, CH_2), 2.48 (d, J = 7.66 Hz, 2H, CH_2), 2.83 (m, 4H, CH_2), 3.76 (d, J = 5.55 Hz, 2H, NCH_2), 4.20 (t, J = 7.67 Hz, 1H, SCH_2), 4.45 (broad, 1H, NH). ^{13}C NMR (CDCl_3 , ppm): 17.4, 18.2 ($\text{C}=\text{C}-\text{CH}_3$), 25.8 ($\text{C}-\text{CH}_2-\text{C}$), 28.3 ($\text{C}(\text{CH}_3)_3$), 30.6 (2 \times SCH_2), 40.1, 43.5 (CH_2), 46.4 ($\text{S}-\text{CH}_2-\text{S}$), 54.2 ($\text{C}-\text{CH}_3$), 128.5, 129.2 ($\text{C}=\text{C}$), 156.0 ($\text{C}=\text{O}$). IR (neat, cm^{-1}): 3358 (m), 2975 (m), 2929 (m), 2914 (m), 2901 (m), 1705 (s), 1507 (m). MS (EI, m/z): 317.1499 (calcd for $\text{C}_{15}\text{H}_{27}\text{NO}_2\text{S}_2$ 317.1483).

***N*-(Isobutyryl)-5,5-dimethoxy-2,3-dimethyl-(*E*)-2-pentenamine (4).** A solution of **3** (0.26 g, 0.82 mmol) in anhydrous MeOH (22 mL) was treated with methanesulfonic acid (0.81 mL, 12.5 mmol), and the mixture was stirred under N_2 for 18 h. The reaction was quenched with aqueous NaHCO_3 (1 N) and then extracted with CH_2Cl_2 (5 \times 10 mL). The combined organic layers were dried with MgSO_4 and concentrated to give 0.17 g (93%) of a yellow oil. ^1H NMR (CDCl_3/TMS , ppm): 1.34 (broad, 2H, NH), 1.78 (m, 6H, CH_3), 1.8–2.2 (m, 2H, CH_2), 2.48 (d, J = 7.66 Hz, 2H, CH_2), 2.8–2.9 (m, 4H, CH_2), 3.27 (s, 2H, NCH_2), 4.22 (t, J = 7.65 Hz, 1H, SCH_2). This material (0.17 g, \sim 0.76 mmol) was dissolved in anhydrous THF (10 mL) under N_2 at 0 $^\circ\text{C}$ and then treated with triethylamine (0.22 mL, 1.52 mmol) and isobutyryl chloride (0.1 mL, 0.95 mmol). A white solid precipitated upon addition of the isobutyryl chloride. After 30 min, the reaction mixture was suction filtered and the filtrate was concentrated. This gave a tan solid (0.20 g) that was dissolved in anhydrous MeOH (5 mL) and then treated with small portions of bis(trifluoroacetoxy)iodobenzene (PIFA) (0.32 g, 0.76 mmol). All solids dissolved quickly, and a slight exotherm resulted upon PIFA addition. After 30 min of stirring under N_2 , the reaction was quenched with 1 N NaHCO_3 and then extracted with Et_2O (3 \times 10 mL). The combined organic layers were dried with Na_2SO_4 and then concentrated. The crude product was purified by silica gel chromatography, eluting with 15% (v/v) EtOAc in hexanes, yielding **4** as a white solid (0.13 g, 64%). Mp (recrystallized from EtOAc and hexanes): 60.0–61.5 $^\circ\text{C}$. ^1H NMR (CDCl_3/TMS , ppm): 1.16 (d, J = 6.90 Hz, 6H, CH_3), 1.71, 1.78 (2 \times m, 6H, $\text{C}-\text{CH}_3$), 2.37 (septet, J = 6.90 Hz, 1H, CH), 2.39 (d, J = 5.68 Hz, 2H, CH_2), 3.34 (s, 6H, OCH_3), 3.89 (d, J = 5.40 Hz, 2H, NCH_2), 4.43 (t, J = 5.54 Hz, 1H, OCHO), 5.31 (broad, 1H, NH). ^{13}C NMR (CDCl_3 , ppm): 17.1 (CH_3), 18.9 (CH_3), 19.7 (2 \times CH_3), 35.7 (CH), 38.3 (CH_2), 42.3 (CH_2N), 53.3 (OCH_3), 103.2 (OCHO), 128.6 ($\text{C}=\text{C}$), 129.6 ($\text{C}=\text{C}$), 176.0 ($\text{C}=\text{O}$). IR (1 mM in CH_2Cl_2 , cm^{-1}): 3442 (w), 1668 (s), 1511 (s), 1447 (m), 1368 (m). MS (EI, m/z): 243.1834 (calcd for $\text{C}_{13}\text{H}_{25}\text{NO}_3$ 243.1844).

NOE Study of Compound 4. An NOE experiment was performed on **4** and its *Z*-isomer using a Bruker AM-500 NMR spectrometer. The automated program NOEDIFF.AU was used for the NOE experiment (using the parameters: D3 = 0.1, S3 = 35L, D1 = 15, D2 = 2, RD = 0, PW = 10.5, DE = 113.8, NS = 8, NE = 8). The results for the *Z*-isomer of **4** are summarized below. NOEs between the vinylmeth-

ylene groups of **4** itself were not observed.



Isobutyryl-ADPA-NHiPr (2). A solution of **4** (97 mg, 0.4 mmol) in THF (1.4 mL) was treated with 1 N HCl (1.4 mL, 1.4 mmol). After stirring for 30 min, the reaction mixture was extracted with CHCl_3 (5 \times 5 mL). The combined organic layers were dried with Na_2SO_4 and then concentrated to yield the aldehyde intermediate (76 mg). ^1H NMR (CDCl_3/TMS , ppm): 1.17 (d, J = 6.81 Hz, 6H, CH_2), 1.69, 1.77 (2 \times m, 6H, $\text{C}=\text{CCH}_3$), 2.36 (septet, J = 6.88 Hz, 1H, CH), 3.19 (s, 2H, CH_2), 3.96 (d, J = 3.55 Hz, 2H, CH_2), 5.40 (broad, 1H, NH), 9.62 (t, J = 2.01 Hz, 1H, HCO). A solution of the crude aldehyde (76 mg, 0.38 mmol) in *t*-BuOH (2 mL) and phosphate buffer (2 mL, 1 N, pH = 4) was treated with 2-methyl-2-butene (0.1 mL, 0.94 mmol) and NaClO_2 (36 mg, 0.40 mmol) and was stirred at room temperature for 30 min. The reaction mixture was extracted with CHCl_3 (10 \times 5 mL), and the combined organic layers were dried with Na_2SO_4 and concentrated to yield the carboxylic acid intermediate (74 mg) as a yellow oil. ^1H NMR (CDCl_3/TMS , ppm): 1.16 (d, J = 6.89 Hz, 6H, CH_3), 1.17, 1.83 (2 \times m, 6H, $\text{C}=\text{CCH}_3$), 2.37 (septet, J = 6.85 Hz, 1H, CH), 3.12 (s, 2H, CH_2), 3.92 (d, J = 5.58 Hz, 2H, NCH_2), 5.52 (broad, 1H, NH). A solution of the crude acid (84 mg, \sim 0.4 mmol) in anhydrous THF (5.2 mL) was treated with *N*-hydroxysuccinimide (61 mg, 0.53 mmol) and dicyclohexylcarbodiimide (DCC) (109 mg, 0.53 mmol), and the mixture was stirred for 2 h under N_2 . Isopropylamine (0.101 mL, 1.2 mmol) was added, and the reaction was stirred for an additional 12 h. The reaction mixture was suction-filtered, and the filtrate was concentrated. The residue was purified by silica gel chromatography eluting with EtOAc, yielding **2** as a white solid (23.9 mg, 28%). Mp (recrystallized from EtOAc and hexanes): 199.0–200.0 $^\circ\text{C}$. ^1H NMR (CDCl_3/TMS , ppm): 1.16 (d, J = 6.88 Hz, 6H, CH_3), 1.13 (d, J = 6.56 Hz, 6H, CH_3), 1.64, 1.85 (2 \times m, 6H, $\text{C}=\text{C}-\text{CH}_3$), 2.37 (septet, J = 6.88 Hz, 1H, CH), 2.99 (s, 2H, CH_2), 3.85 (d, J = 5.39 Hz, 2H, NCH_2), 4.08 (m, 1H, NCH), 5.69 (broad, 1H, NH), 6.08 (broad, 1H, NH). ^{13}C NMR (CDCl_3 , ppm): 16.3 (CH_3), 19.4 (CH_3), 22.5, 19.7 (4 \times CH_3), 41.2 (NCH), 42.9 (CH_2), 43.0 (CH_2), 126.9, 129.6 ($\text{C}=\text{C}$), 169.0, 172.4 ($\text{C}=\text{O}$). IR (1 mM in CH_2Cl_2 , cm^{-1}): 3453 (m), 3330 (m), 1667 (s), 1513 (s), 1467 (m), 1381 (w), 1368 (w). MS (EI, m/z): 254.2009 (calcd for $\text{C}_{14}\text{H}_{26}\text{N}_2\text{O}_2$ 254.1994).

***N*-(Isobutyryl)-5,5-dimethoxy-2,3-diethyl-(*E*)-2-pentenamine.** A slurry of potassium *tert*-butoxide (31.6 g, 258 mmol) and *n*-butyllithium (98.7 mL, 2.6 M in hexane, 258 mmol) in anhydrous pentane (100 mL) was treated dropwise with a solution of 2,3-dimethyl-1,3-butadiene (15 mL, 130 mmol) in anhydrous pentane (50 mL) over 20 min. The slurry was stirred at room temperature for 30 min under N_2 . The stirring was stopped and the resulting orange salt allowed to settle. The pentane was removed over a 2 h period by blowing dry N_2 through the flask. Once the pentane was removed, anhydrous THF (100 mL) was added and the resulting slurry was cooled to -78 $^\circ\text{C}$. The cooled slurry was cannulated into a -78 $^\circ\text{C}$ solution of MeI (16.1 mL, 258 mmol) in anhydrous THF (100 mL) over a 1 h period. The reaction mixture was stirred and allowed to warm to room temperature over 30 min. The reaction mixture was mixed with pentane (250 mL) and then was washed with water (8 \times 100 mL) to remove THF. Pentane in the

resulting yellow liquid was removed by Kugelrohr distillation. The crude material contained significant amounts of pentane and was carried on to the next step without further purification. The yellow oil was dissolved in CHCl_3 at -25°C and then was treated with a solution of bromine (0.55 mL, 11 mmol) in CHCl_3 (10 mL) over a 2 h period. The mixture was stirred an additional 2 h while warming to room temperature. The reaction mixture was concentrated, and the resulting brown material was purified by silica gel chromatography eluting with hexane, yielding 3.76 g of an isomeric mixture (3:1, *E:Z*) of 1,4-dibromo-2,3-diethyl-2-butene as a white solid. $^1\text{H NMR}$ (CDCl_3/TMS , ppm): 1.06, 1.11 ($2 \times \text{t}$, $J = 7.59$ Hz, 6H, CH_3), 2.23, 2.34 ($2 \times \text{q}$, $J = 7.59$ Hz, 4H, CH_2), 4.03, 4.08 ($2 \times \text{s}$, 4H, CH_2Br). MS (EI, m/z): 269.9436 (calcd for $\text{C}_8\text{H}_{14}\text{Br}_2$ 269.9439).

A solution of 1,3-dithiane (2.12 g, 17.6 mmol) in anhydrous THF (40 mL) was cooled to -30°C under N_2 . A solution of *n*-butyllithium (12.0 mL, 1.6 M in hexane, 19.2 mmol) was added dropwise (via cannula) over 40 min. After stirring for an additional 80 min, the solution was added dropwise over 2 h to a solution of 1,4-dibromo-2,3-diethyl-3-(*E*)-butene (3.76 g, 13.9 mmol) in anhydrous THF (30 mL) at -78°C . The resulting yellow solution was stirred for 6 h while being warmed to room temperature. The reaction mixture was quenched with water and then was concentrated to a total volume of 30 mL. The organic layer was separated off, and the aqueous layer was extracted with Et_2O (2×50 mL). The combined organic layers were concentrated in vacuo, and the semisolid residue was taken up in water (35 mL). This mixture was treated with NaN_3 (1.50 g, 23 mmol) and Bu_4NBr (0.50 g, 1.6 mmol), and the two-phase mixture was stirred at 80°C for 10 h. The reaction mixture was cooled, the organic phase was separated, and the aqueous layer was extracted with Et_2O (3×40 mL). The combined organic layers were concentrated to a brown oil. This material was dissolved in THF (20 mL) and water (5 mL) and with triphenylphosphine (5.24 g, 20 mmol). The reaction mixture was stirred at room temperature for 30 h. The THF was removed in vacuo, and the resulting material dissolved in CHCl_3 . This solution was extracted with 1 N HCl (6×30 mL). The combined acidic extracts were made basic with 10 N NaOH, which resulted in the formation of a dark layer at the top of the mixture. The two-phase mixture was extracted with Et_2O (4×50 mL), and the combined organic layers were dried with Na_2SO_4 to yield 1.3 g of amine. The isolated material was a 1:1 mixture of *E*- and *Z*-isomers and was taken to the next reaction without further purification. A stirred solution of the amine (1.3 g, ~ 5.3 mmol) in anhydrous THF (30 mL) was cooled to 0°C under N_2 and then was treated with triethylamine (TEA) (1.12 mL, 8 mmol) and isobutyryl chloride (0.75 mL, 8 mmol). Copious amounts of a white solid precipitated upon addition of the isobutyryl chloride. After 30 min, the reaction mixture was vacuum filtered and the filtrate was concentrated, yielding 1.33 g of crude *N*-(2,3-dimethyl-4-(2,6-dithianyl)-2-pentenyl)-2-methylpropanamide. This material was purified by silica gel chromatography, eluting with 25% (v/v) EtOAc in hexane, yielding a tan solid (0.28 g). $^1\text{H NMR}$ (CDCl_3/TMS , ppm): 0.99 ($2 \times \text{t}$, $J = 7.48$ Hz, 6H, CH_3), 1.15 (d, $J = 6.90$ Hz, 6H, CH_3), 1.8–2.0 (m, 2H, CH_2), 2.12, 2.13 ($2 \times \text{q}$, $J = 7.45, 7.47$ Hz, 4H, CH_2), 2.34 (septet, $J = 6.90$ Hz, 1H, CH), 2.52 (d, $J = 7.78$ Hz, 2H), 2.8–2.9 (m, 4H, SCH_2), 3.88 (d, $J = 6.52$ Hz, 2H, NCH_2), 4.19 (t, $J = 7.53$ Hz, 1H, SCHS), 5.21 (broad, 1H, NH). IR (neat, cm^{-1}): 3281(s), 1640 (s), 1560 (m), 1472 (m), 1458 (m), 1430 (w). MS (EI, m/z): 315.1661 (calcd for $\text{C}_{16}\text{H}_{29}\text{NOS}_2$ 315.1690).

A solution *N*-(2,3-dimethyl-4-(2,6-dithianyl)-2-pentenyl)-2-methylpropanamide (0.21 g, 0.67 mmol) in anhydrous MeOH (10 mL) was treated with small portions of PIFA (0.43 g, 1.01 mmol). All solids dissolved quickly, and a slight exotherm resulted upon PIFA addition. After 30 min of stirring under N_2 , the reaction was quenched with 1 N NaHCO_3 and then was extracted with Et_2O (3×10 mL). The combined organic layers were dried with Na_2SO_4 and concentrated. The crude product was purified by silica gel chromatography, eluting with 50%

(v/v) EtOAc in hexane, to yield 0.18 g of the desired product as a white solid. Mp: $52.0\text{--}53.5^\circ\text{C}$. $^1\text{H NMR}$ (CDCl_3/TMS , ppm): 0.97, 0.98 ($2 \times \text{t}$, $J = 7.41, 7.48$ Hz, 6H, CH_3), 1.15 (d, $J = 6.89$ Hz, 6H, CH_3), 2.09, 2.14 ($2 \times \text{q}$, $J = 7.52, 7.54$ Hz, 4H, CH_2), 2.37 (septet, $J = 6.90$ Hz, 1H, CH), 2.39 (d, $J = 5.73$ Hz, 2H), 3.34 (s, 6H, CH_3), 3.88 (d, $J = 5.73$ Hz, 2H, NCH_2), 4.39 (t, $J = 5.55$ Hz, 1H, OCHO), 5.36 (broad, 1H, NH). $^{13}\text{C NMR}$ (CDCl_3 , ppm): 13.3, 13.8 (CH_3), 19.6 (CH_3), 24.0 (CH_2), 25.2 (CH_2), 34.9 (CH_2), 35.6 (CH), 39.4 (NCH_2), 53.4 (OCH_3), 133.7 (C=C), 135.3 (C=C), 176.7 (C=O); IR (1 mM in CH_2Cl_2 , cm^{-1}): 3442 (w), 1712 (w), 1668 (s), 1509 (m), 1460 (w), 1382 (m), 1370 (w). MS (EI, m/z): 271.2144 (calcd for $\text{C}_{15}\text{H}_{29}\text{NO}_3$ 271.2147).

***N*-Isopropyl-3,4-diethyl-5-(isobutyramido)-(*E*)-3-pentenamide (5).** A solution of *N*-(*E*)-2,3-diethyl-5,5-dimethoxy-2-pentenyl)-2-methylpropanamide (0.17 g, 0.62 mmol) in THF (2.15 mL) was treated with 1 N HCl (2.15 mL, 2.15 mmol). After being stirred for 3 h, the reaction mixture was extracted with CHCl_3 (5×5 mL). The combined organic layers were dried with Na_2SO_4 and were concentrated to yield the aldehyde intermediate as a yellow oil (0.13 g). $^1\text{H NMR}$ (CDCl_3/TMS , ppm): 0.98 (t, $J = 7.52$ Hz, 6H, CH_3), 1.15 (d, $J = 6.87$ Hz, 6H, CH_3), 2.05, 2.16 ($2 \times \text{q}$, $J = 7.56, 7.51$ Hz, 4H, CH_2), 2.38 (septet, $J = 6.89$ Hz, 1H, CH), 3.20 (d, $J = 2.08$ Hz, 2H, CH_2), 3.94 (d, $J = 5.25$ Hz, 2H, CH_2), 5.68 (broad, 1H, NH), 9.61 (t, $J = 2.01$ Hz, 1H, HCO). A solution of the aldehyde (0.13 g, 0.58 mmol) in *t*-BuOH (5 mL) and phosphate buffer (5 mL, 1 N, pH = 4) was treated with 2-methyl-2-butene (0.3 mL, 2.82 mmol), and the mixture was stirred for 30 min. The reaction mixture was extracted with CHCl_3 (10×10 mL), and the combined organic layers were dried with Na_2SO_4 . Concentration of the organic layers yielded the desired carboxylic acid intermediate as a yellow semisolid (0.13 g). $^1\text{H NMR}$ (CDCl_3/TMS , ppm): 0.98 (t, $J = 7.50$ Hz, 6H, CH_3), 1.15 (d, $J = 6.88$ Hz, 6H, CH_3), 2.06, 2.18 ($2 \times \text{q}$, $J = 7.53, 7.53$ Hz, 4H, CH_2), 2.38 (septet, $J = 6.87$ Hz, 1H, CH), 3.13 (s, 2H, CH_2), 3.90 (d, $J = 5.00$ Hz, 2H, CH_2), 5.68 (broad, 1H, NH), 6.95 (broad, 1H, COOH). A solution of the acid (136 mg, ~ 0.57 mmol) in anhydrous CH_2Cl_2 (5.2 mL) was treated with *N*-hydroxysuccinimide (89 mg, 0.77 mmol) and DCC (159 mg, 0.77 mmol), and the mixture was stirred for 2 h under N_2 . Isopropylamine (0.15 mL, 1.7 mmol) was added, and the reaction was stirred for an additional 12 h. The reaction mixture was filtered, and the filtrate was concentrated. The resulting residue was purified by silica gel chromatography eluting with 50% (v/v) EtOAc in hexane, yielding **5** (76 mg, 44%) as a white solid. Mp (recrystallized from EtOAc and hexane): $159.0\text{--}161.0^\circ\text{C}$. $^1\text{H NMR}$ (CDCl_3/TMS , ppm): 0.97 (t, $J = 7.49$ Hz, 6H, CH_3), 1.13 (d, $J = 6.63$ Hz, 6H, CH_3), 1.16 (d, 6.95 Hz, 6H, CH_2), 2.03, 2.23 ($2 \times \text{q}$, $J = 7.57, 7.53$ Hz, 4H, CH_2), 2.35 (septet, $J = 6.87$ Hz, 1H, CH), 3.01 (s, 2H, CH_2), 3.88 (d, $J = 5.27$ Hz, 2H, NCH_2), 4.07 (m, 1H, NCH), 5.56 (broad, 1H, NH), 6.00 (broad, 1H, NH). $^{13}\text{C NMR}$ (CDCl_3 , ppm): 13.1 (CH_3), 13.4 (CH_3), 22.5, 23.2 ($4 \times \text{CH}_3$), 23.2, 26.3 (CH_2), 35.6 (CH), 39.7, 39.9 (CH_2), 41.2 (NCH), 130.9, 135.6 (C=C), 169.6, 177.2 (C=O). IR (1 mM in CH_2Cl_2 , cm^{-1}): 3450 (w), 3439 (w), 3412 (w), 3332 (w), 1711 (w), 1669 (s), 1650 (m), 1605 (w). MS (EI, m/z): 282.2295 (calcd for $\text{C}_{16}\text{H}_{30}\text{N}_2\text{O}_2$ 282.2209).

Acknowledgment. This research was supported by the National Science Foundation (CHE-9622953). NMR spectrometers were purchased through Grants NSF CHE-8813550 and NIH 1 S10 RR04981.

Supporting Information Available: Text describing synthetic protocols and characterization for molecules not discussed in the Experimental Section (PDF). This material is available free of charge via the Internet at <http://pubs.acs.org>.

JA9824526